Article

Journal of
Nanoscience and Nanotechnology
Vol. 15, 8907–8911, 2015
www.aspbs.com/jnn

Enhanced Output Power of PZT Nanogenerator by Controlling Surface Morphology of Electrode

Woo-Suk Jung[1, †], Won-Hee Lee[2, †], Byeong-Kwon Ju[3], Seok-Jin Yoon[1], and Chong-Yun Kang[1, 4, *]

[1] *Electronic Materials Research Center, Korea Institute of Science and Technology (KIST), Hwarangno 14-gil 5, Seongbuk-gu, Seoul 136-791, Korea*
[2] *Probe Development Lab, Samsung Medison, Teheran-ro 108-gil, Gangnam-gu, Seoul 135-851, South Korea*
[3] *Display and Nanosystem Laboratory, School of Engineering, Korea University, Seoul 136-713, Republic of Korea*
[4] *KU-KIST Graduate School of Converging Science and Technology, Korea University, 145, Anam-ro, Seongbuk-gu, Seoul 136-701, Korea*

Piezoelectric power generation using $Pb(Zr,Ti)O_3$(PZT) nanowires grown on Nb-doped $SrTiO_3$(nb:STO) substrate has been demonstrated. The epitaxial PZT nanowires prepared by a hydrothermal method, with a diameter and length of approximately 300 nm and 7 μm, respecively, were vertically aligned on the substrate. An embossed Au top electrode was applied to maximize the effective power generation area for non-uniform PZT nanowires. The PZT nanogenerator produced output power density of 0.56 $\mu W/cm^2$ with a voltage of 0.9 V and current of 75 nA. This research suggests that the morphology control of top electrode can be useful to improve the efficiency of piezoelectric power generation.

Keywords: PZT, Nanostructure, Hydrothermal, Nanogenerator, Energy Harvesting.

1. INTRODUCTION

With an increasing concern about global warming and renewable energy, piezoelectricity generated from piezoelectric materials has received a lot of attentions in research and development for converting energy from the environment, and various piezoelectric materials are being studied for harvesting energy such as a ZnO, $BaTiO_3$, $NaNbO_3$, and GaN.[1–7] Such systems using those materials can be applied for various advanced devices such as mobile electronics, muscle, self-powered wireless sensor network and body implantable devices.[8–10] In addition, advances in technology bring about smaller and lighter electronic devices, and energy harvester should be corresponded to this trend.

Thus, nanostructures for energy harvesting devices are rising as alternatives with great prospects against chemical batteries due to its flexibility, portability, and wearability. The piezoelectric properties of one-dimensional piezoelectric nanostructures are currently attracting great interest due to their potentials for numerous applications and also being applied for the piezoelectric nanogenerators. These nanostructures have also shown excellent performance for energy harvesting.[11–17] Among the various piezoelectric materials, $Pb(ZrTi)O_3$ is the most promising complex oxide material with an extraordinary high dielectric constant, a large hysteresis, and an excellent piezoelectric coefficient, which can be readily incorporated with energy harvesting devices. In comparison with the polycrystalline PZTs, it has been reported that the single crystalline PZT nanowires (NWs) exhibit higher piezoelectric constants and greater electromechanical coupling coefficients up to two orders of magnitude higher than those of ZnO NWs as well as 6–12 times higher than that of PZT cantilever.[17–19] Epitaxial growth of such crystals depends on both the use of rigid and inorganic host substrates and the high temperature deposition process, which lead not only to increase manufacturing cost but also to make integration with soft materials difficult. The hydrothermal technique has become one of the most important tools for advanced materials processing owing to its advantages in the fabrication process of nanostructure materials for a

*Author to whom correspondence should be addressed.
†These two authors contributed equally to this work.

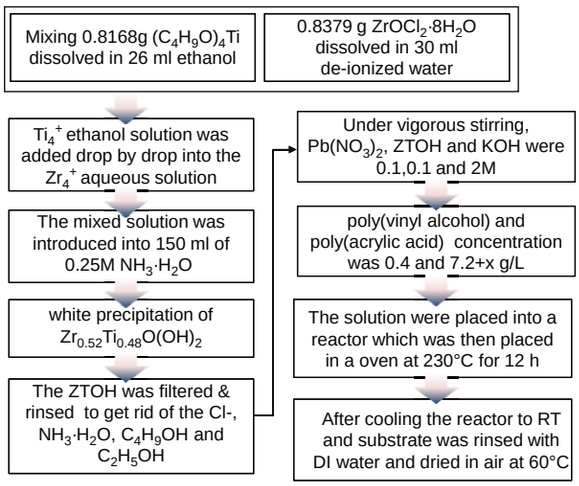

Figure 1. Hydrothermal solution procedure to synthesize PZT nanowires.

wide variety of technological applications. Hydrothermal epitaxy is a technique that uses aqueous chemical reactions to synthesize heteroepitaxial NWs on structurally similar single-crystal substrates under an elevated pressure and a low processing temperature (90–200 °C).[20] It is therefore demonstrated that this method provides a low cost as well as a low temperature process to produce high-quality single-crystal NWs. Recently, Xu et al. successfully grew PZT NWs onto Nb:STO by hydrothermal method and then measured the electrical properties.[17] In Wang's group, the generator using PZT NWs produces ~0.7 of peak voltage and 4 $\mu A/cm^2$ of peak current density.[21] However, the height of grown NWs was not uniform, and only a few percent of them were actively generating electricity, and output current is relatively low compared to output voltage. Therefore, to increase the output power, it is necessary to make further improvements for the feature of NWs since zigzag or embossed top electrode structures can lead to higher current generation.[11]

Here, we demonstrate piezoelectric power generation using $Pb(Zr,Ti)O_3$(PZT) nanowires grown on $Nb:SrTiO_3$ substrate. To increase output power from PZT nanowires, a 3D embossed Au electrode has been employed.

2. EXPERIMENTAL DETAILS

The mixed surfactant system to effectively promote anisotropic growth and the formation of single crystalline PZT nanowires has been proposed. Figure 1 shows the hydrothermal process to synthesize PZT nanowires. The hydrothermal solution used for the NW growth was prepared by dissolving tetrabutyl titanate ($[C_4H_9O]_4Ti$) in ethanol to form a 0.15 M solution and then zirconium oxychloride ($ZrOCl_2$-$8H_2O$) was dissolved in de-ionized (DI) water to form a 0.08 M solution. The mixture of both the solutions resulted in the corecipitation of $Zr_{0.52}Ti_{0.48}O(OH)_2$(ZTOH). After many times ringing with DI water, lead nitrade [$Pb(NO_3)_2$] and potassium hydroxide (KOH) were introduced into the ZTOH. The PVA and PAA with the concentration of 0.4 and 7.2 g/L, respectively, were added under vigorous stirring in order to form the final hydrothermal solution with a 50 mL total volume. Single crystalline Nb-doped $SrTiO_3$ (Nb:STO) substrate was chosen for both the epitaxial growth owing to their small lattice mismatch with PZT (lattice constants, *a*: PZT, 4.03–4.07 Å; $SrTiO_3$, 3.905 Å) as well as for the bottom electrode.[22] During the nucleation and growth of PZT nanowires, the poly(vinyl alcohol) and poly(acrylic acid) perform as the surfactants.[17, 20] The substrate and hydrothermal solution were placed into a stainless steel autoclave with a Teflon liner, which was then placed in a vacuum oven at 200 °C for 12 h. After cooling the autoclave at room temperature, the substrate with PZT crystals was rinsed with DI water and dried in air at 60 °C for 3 h. Figure 2 shows the cross-sectional scanning electron microscopy (SEM) image of the vertically aligned PZT nanowires on the Nb:STO substrate and SEM image of the PZT nanowires at a tilt angle of 20°. The length of the nanowires is around 5~7 μm and diameters are ranged from 200 to 500 nm.

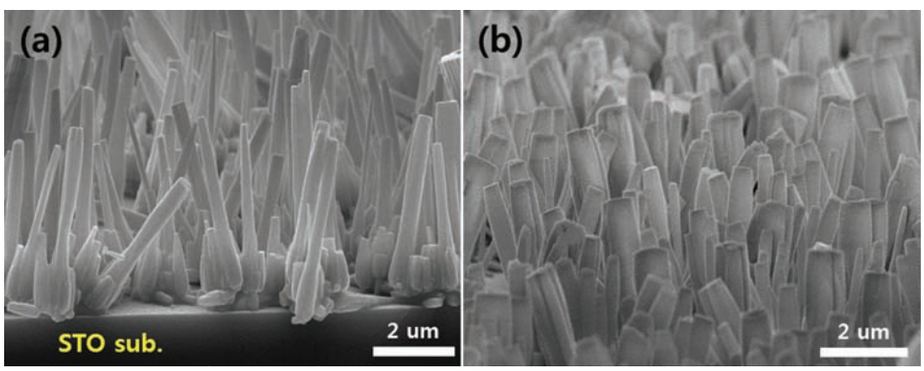

Figure 2. SEM images of PZT nanowires. (a) Cross-sectional image of the PZT nanowires grown on Nb:STO substrate and (b) SEM image of the PZT nanowires at a tilt angle of 20°.

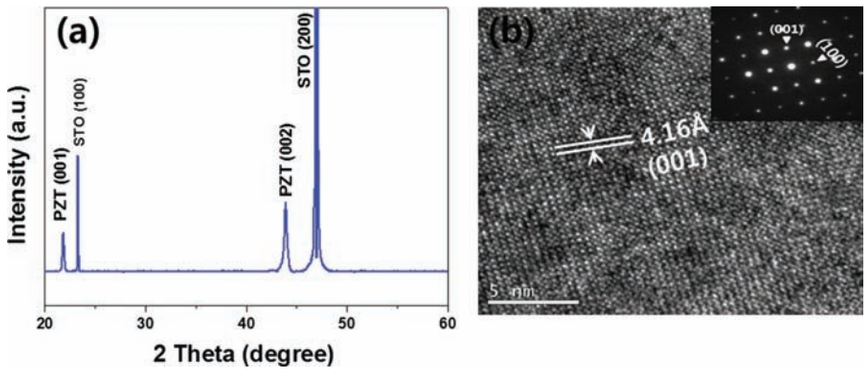

Figure 3. (a) X-ray diffraction pattern and (b) HRTEM image and electron diffraction pattern for the as-grown PZT nanowire array.

3. RESULTS AND DISCUSSION

Structural characteristics of the PZT NWs grown on the Nb:STO substrate were analyzed by an XRD as shown in Figure 3(a), As the (100)-oriented Nb:STO substrate affected to the growth of PZT NWs, only the peaks corresponding to the perovskite PZT (001) orientations were observed, whereas any other peaks presenting mis-oriented grains such as (110) and (111) orientations or metastable pyrochlore phases were recognized. A high-resolution transmission electron microscopy (HRTEM) analysis for a single PZT nanowire shows that the as-synthesized nanowires have a tetragonal phase consisted of single crystalline PZT with a (001) growth direction are shown in Figure 3(b). To fabricate PZT nanogenerator, electrical poling for the nanowires was conducted by applying an external electrical field of 100 KVcm-1 by the Corona poling technique.

To improve the output power of the nanogenerator at a given NWs, the current density should increase by enlarging the active area participating in the electrical generation. Therefore, we focused on the morphology control of top electrode to increase the number of NW contributing the electrical generation. For the fabrication of embossed Au electrode, an aqueous suspension of 50-nm-diameter polystyrene (PS) beads (Polysciences, Warrington, U.S.) was used to prepare close-packed monolayer bead templates. A drop of the polystyrene bead suspension was then pipetted onto the SiO_2 substrate. Spin-coating of the polystyrene beads was done at 2000 rpm for 3 s with a ramp-up time of 1 s. The sample was dried for 1 h in a drybox at room temperature. And then, Au/Ti layer (50/10 nm) was deposited on SiO_2 substrate using a DC sputtering, and then heat-treated at 600 °C for 1 h to remove PS beads. Figure 4 shows PS beads on the substrate and embossed Au layer with 50 nm of thickness, respectively. As shown in Figure 1, the morphology of flat-typed electrode is not proper as the top electrode because of the non-uniform PZT NWs, whereas the embossed Au layer provides much more electron paths for NWs with various heights to contribute the improvement of current density.

The morphological effect of the top electrode was analyzed by measuring the output current excited from the nanogenerator. When the PZT NWs array is subject to uniaxial compressive force, piezoelectric fields are created inside the NWs and consequently free electrons flow across the external force, generating voltage and current peaks. Once the external force is released, the electrons flow in the opposite direction.

Figures 5(a)–(b) demonstrates the output voltage and current pulses excited by the PZT nanogenerator with a flat Au top electrode generally prepared under periodical compressing and releasing. The generated outputs including both the positive and negative polarities are

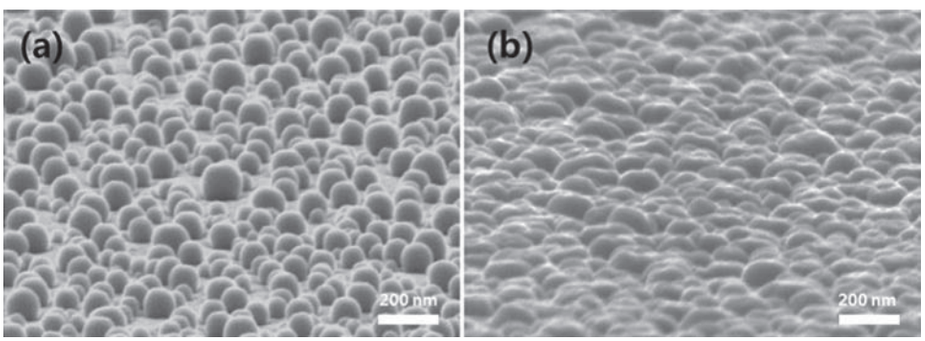

Figure 4. SEM images of top electrodes (a) with polystyrene beads and (b) with embossed Au layer on PS beads.

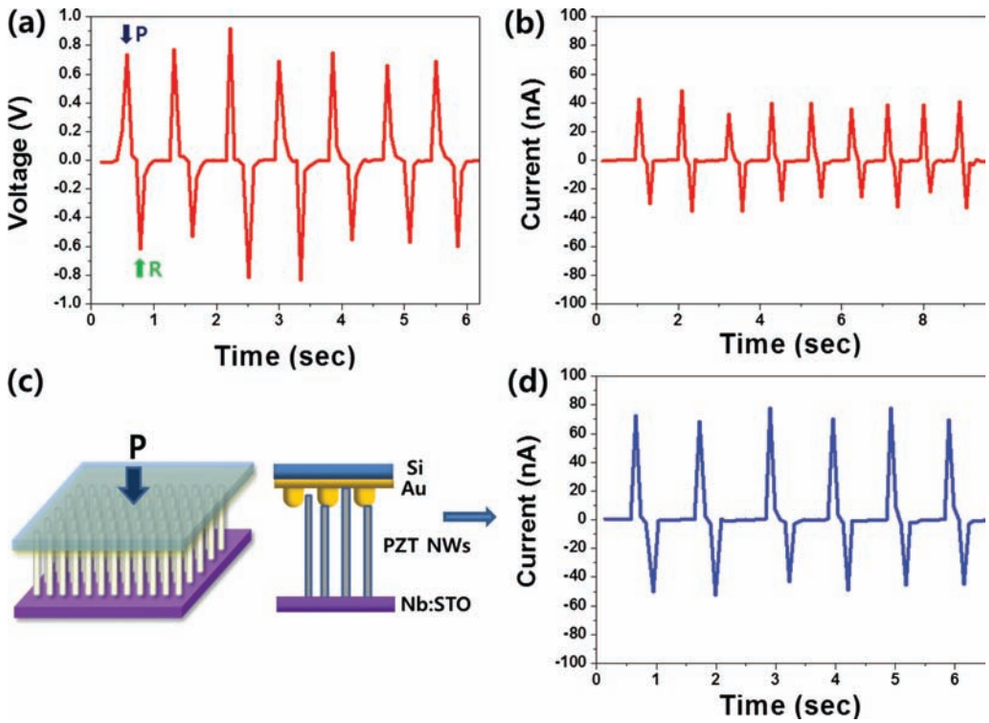

Figure 5. Electrical properties of the PZT nanogenerator with the agglomerated Au top electrode. (a) output voltage and (b) output current of PZT nanogenerator. (c) and (d) shows the schematic image of PZT nanogenerator with the embossed Au electrode and its enhanced output current, respectively.

observed. The negative output distribution is generated due to the reverse flowing carriers when the external force was removed and the piezoelectric potential vanished. In case of the flat top electrodes, peak output voltage of 0.9 V and peak current of 40 nA are observed. For the PZT nanogenerator with the embossed Au top electrode, the peak output current increases up to 75 nA whereas the output voltage is the same as the previous one due to the same length of the NWs, as shown in Figure 5(d). This is because the embossed electrode provides more active area that can contact with PZT nanowires as shown in Figure 5(c). It can be obviously explained from the electrical performance that much more NWs could contribute the electrical generation since the embossed top electrode helped the NWs of various sizes make metal/piezo-semiconductor schottky contact. The output power density of 0.56 μW/cm^2 was finally obtained, implying great improvement of current density by employing the embossed top electrode. Since it is hard to grow the PZT NWs perpendicular to the substrate compared to the ZnO NWs, the morphology control of top electrode can be useful for the non-uniform NWs.

4. CONCLUSION

In summary, we have fabricated epitaxial lead zirconate titanate (PZT) nanowires on the single-crystal Nb:STO substrate by the hydrothermal method. The nanowires exhibit with a diameter and length of approximately 300 nm and 7 μm, respectively. To enhance output current of the PZT nanogenerator, we controlled the morphology of the electrode surface in order to provide electron paths effectively. The peak current reached to 75 nA using the embossed Au top electrode, it is almost 2 times higher than the flat top electrode, whereas the peak voltage of 0.9 V kept as the same voltage generated by the flat-typed electrode because the output voltage is dependent on the length of NWs. It is obviously seen that the current density of the NG can be controlled by means of the morphology of top electrode because of the increase of the active contact area for non-uniform height of the PZT nanowires. The results of experimental investigation will be used for an important step toward the design and optimization of NG.

Acknowledgment: This work was supported by the Energy Technology Development Project (KETEP) grant funded by the Ministry of Trade, Industry and Energy, Republic of Korea (Piezoelectric Energy Harvester Development and Demonstration for scavenging Energy from Road Traffic System, project No. 20142020103970) and the Institutional Research Program of the Korea Institute of Science and Technology (2E25440) and KU-KIST Research Program of Korea University (R1309521).

References and Notes

1. J. P. Holdren, *Sustainability and Energy, Science* 315, 721 (**2007**).
2. S. H. Lee, W. B. Ko, and J. Hong, *J. of Nanosci and Nanotechn.* 14, 9319 (**2014**).

3. G. Zhu, A. C. Wang, Y. Liu, Y. Zhou, and Z. L. Wang, *Nano Lett*. 12, 3086 (**2012**).
4. K. I. Park, S. Xu, Y. Liu, G. T. Hwang, S. J. L. Kang, Z. L. Wang, and K. J. Lee. *Nano Lett*. 10, 4939 (**2010**).
5. J. H. Jung, M. B. Lee, J. I. Hong, Y. Ding, C. Y. Chen, L. J. Chou, and Z. L. Wang. *ACS Nano.* 5, 10041 (**2011**).
6. L. Lin, C. H. Lai, Y. Hu, Y. Zhang, X. Wang, C. Xu, R. L. Snyder, L. J. Chen, and Z. L. Wang. *Nanotechn*. 22, 475401 (**2011**).
7. J. Kim and J. H. Koh, *J. of Nanosci. and Nanotechn*. 15, 2360 (**2015**).
8. C. Pan, H. Wu, C. Wang, B. Wang, L. Zhang, Z. Cheng, P. Hu, W. Pan, Z. Zhou, X. Yang, and J. Zhu. *Adv. Mater*. 20, 1644 (**2008**).
9. B. J. Hansen, Y. Liu, R. Yang, and Z. L. Wang. *ACS Nano.* 4, 3647 (**2010**).
10. Z. Li, G. Zhu, R. Yang, A. C. Wang, and Z. L. Wang. *Adv. Mater*. 22, 2534 (**2010**).
11. X. D. Wang, J. H. Song, J. Liu, and Z. L. Wang. *Science* 316, 102 (**2007**).
12. S. Xu, Y. Qin, C. Xu, Y. G. Wei, R. S. Yang, and Z. L. Wang. *Nature Nanotechn*. 5, 366 (**2010**).
13. Z. Y. Wang, J. Hu, P. A. Suryavanshi, K. Yum, and M. F. Yu, *Nano Lett*. 7, 2966 (**2007**).
14. X. Chen, S. Y. Xu, N. Yao, and Y. Shi. *Nano Lett*. 10, 2133 (**2010**).
15. C. Chang, H. V. Tran, J. B. Wang, Y. K. Fuh, and L. W. Lin. *Nano Lett.* 10, 726 (**2010**).
16. P. M. Rorvik, T. Grande, and M. A. Einarsrud, *Adv. Mater*. 23, 4007 (**2011**).
17. S. Xu, B. J. Hansen, and Z. L. Wang, *Nature Comm*. 1, 93 (**2010**).
18. J. Wang, C. S. Sandu, E. Colla, Y. Wang, W. Ma, R. Gysel, H. J. Trodahl, N. Setter, and M. Kuball. *Appl. Phys. Lett*. 90, 133107 (**2007**).
19. X. Chen, S. Xu, N. Yao, W. Xu, and Y. Shi. *Appl. Phys. Lett*. 94, 253113 (**2009**).
20. G. Xu, Z. Ren, P. Du, W. Weng, G. Shen, and G. Han. *Adv. Mater*. 17, 407 (**2005**).
21. S. Xu, B. J. Hansen, and Z. L. Wang, *Nature Comm*. 93, 1098 (**2010**).
22. Z. X. Zhu, J. F. Li, F. P. Lai, Y. Zhen, Y. H. Lin, C. W. Nan, and L. Li. *Appl. Phys. Lett*. 91, 222910 (**2007**).

Received: 5 December 2014. Accepted: 27 January 2015.